

## Three Dimensional Secondary Vortexes in the Wake past a Circular Cylinder Using High Order Scheme

Tae Soo Kim<sup>1</sup>, Pa Ul Mun<sup>1</sup>, Myung Kuk Lee<sup>1</sup> and Jae Soo Kim<sup>1 2</sup>

**keywords:** Three Dimensional secondary vortexes, Optimized High-Order Compact Scheme, Vortex Shedding, OpenMP Parallelized Computation

### Introduction

While the research for flow over a circular cylinder has been actively carried out up to the present, it has been known that the flow has not been clarified even now. Various complex flow and aero-acoustic characteristics exist around a circular cylinder such as flow separation, wake and pressure wave propagation [1]. The flow is symmetric with respect to the front and back if the Reynolds Number is less than 45. If the Reynolds Number is higher, vortex shedding will occur in the rear of cylinder because abnormal flow will occur. This vortex shedding becomes the main cause of vibration, noise and periodic lift and drag on the cylinder. Norberg[1] compiled the theoretical, experimental and numerical research results for a circular cylinder flow and analyzed the flow characteristic according to the Reynolds number. He showed that there was a considerable difference in characteristics between experimental and numerical analysis results up to the present. As the Reynolds number increases, three dimensional instability increases in the wakes, and this becomes the cause for increase in lift, drag and Reynolds stress. Because of the pressure change, Karman vortex will occur periodically and the periodic characteristic of lift and drag will be generated [2]. Williamson [3] showed that two dimensional vortex shedding occurs when the Reynolds Number is less than 180. When it is greater than this value, he showed that unstable three dimensional vortex shedding will appear as Mode A and Mode B form.

In this paper, research was carried out for wake flow over a circular cylinders by using high order, high resolution techniques that are used in two dimensional aero-acoustic analysis[4]. While theoretical equations and experiments were mainly used for the analysis of aero- acoustic in the past [5], a variety of research is being carried out for the mutual interference between flow and acoustics by using high order computation techniques in recent times. Numerical instability occurs if nonlinear discontinuous wave is computed with a high order, high resolution technique. The artificial dissipation model proposed by Kim&Lee [6] was applied to three dimensional flows to remove the numerical instability. Numerical analysis using the high order technique requires a long computation time and a large memory capacity. Therefore, in order to improve the processing time, OpenMP parallel

---

<sup>1</sup>Department of Aerospace Engineering, Chosun University, 375 Seosuk-dong, Dong-gu, Kwang-Ju, 501-759, Republic of Korea

<sup>2</sup>corresponding author, E-mail:jsckim@chosun.ac.kr, Tel) 82-62-230-7080

processing method was used. For the numerical result, the periodic characteristic of Strouhal Number due to vortex shedding was comparatively analyzed with other experiment values and two dimensional numerical results. The characteristics of secondary vortex were analyzed for the three dimensional flow characteristic of wake.

### Governing Equations and Numerical Analysis Method

The three dimensional unsteady compressible Reynolds Averaged Navier-Stokes equation was transformed into a general coordinates, as Eq.(1). The detailed equations are as shown in the reference [7].

$$\frac{\partial \hat{Q}}{\partial t} + \frac{\partial \hat{E}}{\partial \xi} + \frac{\partial \hat{F}}{\partial \eta} + \frac{\partial \hat{G}}{\partial \zeta} = \frac{\partial \hat{E}_V}{\partial \xi} + \frac{\partial \hat{F}_V}{\partial \eta} + \frac{\partial \hat{G}_V}{\partial \zeta} \quad (1)$$

For a high order, high resolution numerical technique, OHOC (Optimized High-Order Compact) numerical technique used by Kim& Lee [4] in two dimensional aero-acoustic analyses was applied to three dimensional flows. For numerical differentiation, an implicit method using 7 node points was used, as shown in Eq.(2). The coefficients are as shown in reference [4]. In order to maintain high resolution in time direction, a fourth order Runge-Kutta explicit method was used [8].

$$\beta f'_{i-2} + \alpha f'_{i-1} + f'_i + \alpha f'_{i+1} + \beta f'_{i+2} = \frac{1}{h} \sum_{m=1}^3 a_m (f_{i+m} - f_{i-m}) \quad (2)$$

While it is possible to obtain high resolution with OHOC technique, dissipation and diffusion errors occur. These errors affect numerical stability significantly, because the wave characteristic cannot be accurately reproduced unlike an upwind scheme due to the characteristics of central difference method. In order to reduce this error and increase the stability of numerical scheme, the adaptive nonlinear artificial dissipation model proposed by Kim&Lee [6] was applied to the three dimensional flow.

The computation domain was set up to be 200 and  $(\pi D/2, \pi D, 2\pi D)$  times the diameter D in the radial direction and the spanwise direction, respectively. The number of O-type grid system  $201 \times 141 \times (20, 40, 60)$  was used. Fig.1 shows the sample grid system on the center section of numerical domain. In most of research for compressible flow, the wave reflection from the boundary is suppressed by using a non-reflecting characteristic method. However, for the high resolution technique, the wave reflection is suppressed with numerical dissipation by a wide area of buffer zone, because the wave reflection is not sufficiently suppressed even though a non-reflecting condition is used. In this paper, a wide numerical computation zone was set up and a coarse grid was used in the distant boundary region. Therefore, while

the numerical computation domain was set up wider than the methods with non-reflective characteristic condition, the boundary conditions were given very simply for non-reflecting condition.

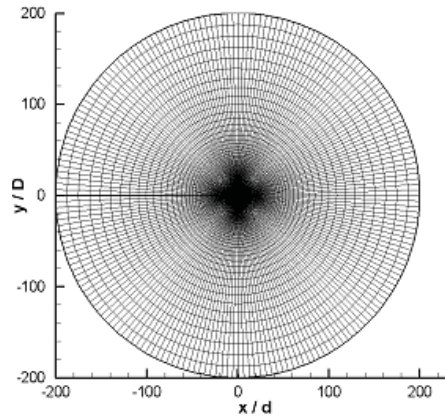


Figure 1: Grid Mesh System for computation of circular cylinder flow

For the parallel processing technique, the OpenMp method uses a shared memory based on a thread and allows relatively easy programming, the MPI method is carried out with independent memory in each processor with data communication, and the Cluster OpenMP has the advantages of both. OpenMP was mainly used in this research because of CPU time consumption for data communication.

### Result and Discussion

In Figure 2, the Strouhal number ( $St = fD/U_\infty$ ) of lift coefficient was compared with other numerical results and experiment values, for the variations of Reynolds number and spanwise length. The Reynolds number ranges from 300 to 1000, which belongs to mode B referred by Williamson [3]. The results seriously differed from the 2- dimensional result of Williamson [3]. Even though the results in the range of mode B Reynolds number have a little difference with Williamson [3], they very closely agree with the Leweke [9]. There are no significant differences for the variation of spanwise length.

Figure 3 shows the vortex shedding for one period on the central cross section of z-axis. A primary vortex occurs, develops strongly and flows downstream. Then a second vortex in the primary vortex occurs. It can be seen that this second vortex vanishes by being strongly pushed out by the primary vortex from the opposite side. Finally, the original primary vortex is shed toward downstream. Such a process completely shows the periodic characteristic of Karman vortex. It also shows the dissipation of vortex strength as it flows downstream.

For the variation of spanwise length, the distributions of secondary vortex show

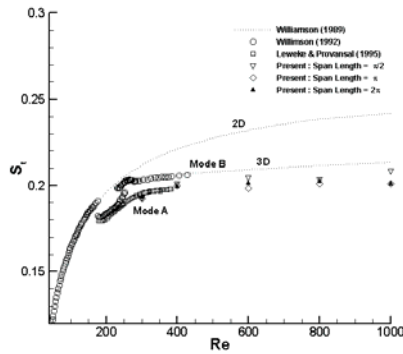


Figure 2: Relationship between St and Re

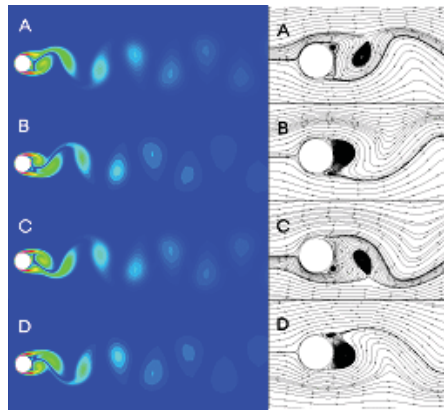


Figure 3: Vorticity and streamline Patterns from 1 period at Re=300

in Figure 4 for the case of Reynolds number of 1000. In the cases of spanwise length of  $\pi D/2$ , the distribution of secondary vortices are parallel. However, the three dimensional effects are shown in the results of spanwise length of  $\pi D$  and  $2\pi D$ . The wave lengths of secondary vortices are shown in Figure 4 for the variation of spanwise length and Reynold number. For the case of spanwise length of  $\pi D/2$ , the results are very lower than Williamson [3]. For the case of spanwise length of  $2\pi D$ , the results more closely agree with Williamson [3]. However, the results differ from Williamson [3] in the range of low Reynolds number near to mode A range. The reason seems the numerical dissipation. Therefore, the spanwise length is required over  $2\pi D$  and the numerical dissipation is suppressed for the accurate three dimensional effects.

### Conclusion

The unsteady three dimensional compressible Reynolds averaged Navier Stokes



Figure 4: B-mode vortex shedding: comparison of streamwise components of vortexes for  $\pi d/2$ (top),  $\pi d$ (middle),  $2\pi d$ (bottom) at  $Re=1000$

equation was numerically computed to analyze the secondary vortexes in wakes past a circular cylinder by applying the OHOC technique, a high order and high resolution numerical technique. To increase the computation speed for the large amount of numerical computations, a OpenMP parallel processing method was used. Since a non-reflective characteristic boundary condition needs a large buffer zone for a high order technique, it is not efficient. Therefore, in this research, while the numerical computation domain was set up wider than the methods with non-reflective characteristic condition, the very simple boundary conditions were used. For the variations of Reynolds number of mode B and spanwise length, Strouhal number of lift was compared with other two dimensional numerical computation results and experiment values. Karman vortex shedding characteristic, three dimensional vortex shedding and secondary vortex characteristics were analyzed. When the spanwise length is over  $2\pi D$ , three dimensional effects are more accurately analyzed. Even though there are secondary vortexes in the range of low Reynolds number or short spanwise length, the secondary vortexes flow down in a parallel direction. Therefore, there are no three dimensional effects in the results of lift and drag coefficients.

### References

1. Norberg, C. (2003) : Fluctuating Lift on a Circular Cylinder, Review and new Measurements., *J. of Fluids and Structures*, Vol. 17, p.57-96.
2. William K. Blake (1986) : Mechanics of Flow-Induced Sound and Vibration,

ACADEMIC PRESS. INC.

3. Williamson, C.H.K. (1996) : Three Dimensional wake transition., *J. Fluid Mech.*, Vol.328, p. 345-407.
4. Kim, J.W. and Lee,D.J. (1996) : Optimizd Compact Finite Difference Schemes with maximum Resolution, *AIAA Journal*, Vol.34, No.5, p. 887-893.
5. Lighthill, M. J. (1952) : On Sound Generated Aerodynamically: I.General Theory, *Proceedings of the Royal Society*, London, A221(1107), p. 564-587.
6. Kim, J.W. and Lee, D.J. (1999) : Adaptive Nonlinear Artificial Dissipation Model for Computational Aeroacoustics, *3rd CAA Workshop on Benchmark Problems*, USA.
7. C.H. Woo, J.S.Kim, and K.H.Lee (2006) : Analysis of Two- and three-Dimensional Supersonic Turbulence Flow around Tandem cavities, *Journal of Mechanicals Science and Technology(KSME Int.J.)*, Vol.20, No.8, p. 1256-1265.
8. Hoffmann,K.C. and Chiang S.T. (1993) :Computational Fluid Dynamics for Engineers, Engineering Education System, USA,
9. T. Leweke, Williamson, C.H.K. (1998) : Three-dimensional instabilities in wake transition., *J. mech. B/Fluids*, vol.17, p. 571-586.